Received March 24, 2017, accepted April 16, 2017, date of publication April 19, 2017, date of current version May 17, 2017.

Digital Object Identifier 10.1109/ACCESS.2017.2695586

Achievable Rates of UAV-Relayed Cooperative Cognitive Radio MIMO Systems

LOKMAN SBOUI[1], (Student Member, IEEE), HAKIM GHAZZAI[2], (Member, IEEE), ZOUHEIR REZKI[3], (Senior Member, IEEE), AND MOHAMED-SLIM ALOUINI[1], (Fellow, IEEE)
[1]King Abdullah University of Science and Technology, Thuwal 23955, Saudi Arabia
[2]Qatar Mobility Innovations Center, Qatar University, Doha 210531, Qatar
[3]University of Idaho, Moscow, ID 83844 USA

Corresponding author: Lokman Sboui (lokman.sboui@kaust.edu.sa)

Part of this paper was presented at the 13th International Wireless Communications and Mobile Computing Conference (IWCMC'17), Valencia, Spain, June, 2017 [1].

ABSTRACT We study the achievable rate of an uplink MIMO cognitive radio system where the primary user (PU) and the secondary user (SU) aim to communicate to the closest primary base station (BS) via a multi-access channel through the same unmanned aerial vehicle (UAV) relay. The SU message is then forwarded from the primary BS to the secondary network with a certain incentive reward as a part of the cooperation protocol between both the networks. A special linear precoding scheme is proposed to enable the SU to exploit the PU free eigenmodes. We analyze two scenarios in which the UAV relay gain matrix is either fixed or optimized. We derive the optimal power allocation that maximizes the achievable rate of the SU respecting power budget, interference, and relay power constraints. Numerical results highlight the cognitive rate gain of our proposed scheme with respect to various problem parameters. We also highlight the effect of UAV altitude on the SU and PU rates. Finally, when the relay matrix is optimized, we show that the PU rate is remarkably enhanced and that the SU rate is only improved at high-power regime.

INDEX TERMS MIMO space alignment, relay matrix optimization, UAV-based communication, underlay cognitive radio.

I. INTRODUCTION

Given the increasing demand in wireless communications and the emergence of the concept of Internet of Things (IoT), the upcoming fifth generation of wireless networks (5G) is expected to radically exceed the performances of the current deployed forth generation (4G). It is expected that the data rate will be 1000 times the 4G data rate [2]. In addition, the latency is expected to be reduced from 15ms, in the 4G, to 1 ms in the 5G [2]. Also, the energy consumption of 5G networks will be reduced by up to 90% compared to the 4G [3].

In order to reach these performances, multiple key enabling technologies are proposed, e.g., networks densification, advanced multiple-Input multiple-output (MIMO) communication, spectrum sharing using cognitive radio (CR) techniques, the use of the unmanned aerial vehicles (UAVs), etc. The UAVs were proposed to operate as a part of the wireless networks to achieve some of the 5G requirements. With their reduced size, the UAVs can be used as potential relays in the 5G networks [4]. As the 5G applications are extended beyond classical cellular networks, the UAVs are a key component that will enable the next generation of the wireless networks with various new applications such as products delivery, police patrolling, infrastructure inspections, agriculture monitoring; to name a few [5], [6].

A common use of the UAV is relaying the wireless communications. In the literature, early studies on cooperative relays were presented in [7] and [8]. The relaying concept consists in deploying additional nodes in the network that are responsible in retransmitting the received signal to the destination to enhance reliability and reduce the communication cost in terms of power [9], [10]. Relaying is very efficient in cell edge cases in which the source transmission requires high power that may lead to high interference thus, detrimentally affecting the cell throughput. In many cases, relays need to be implemented rapidly and temporarily, for instance, in natural disasters or crowded events [11], [12].

Adopting UAV-based relays is considered an efficient and fast way to deploy or extend wireless networks. Consequently, cooperative UAV relays represent an efficient solution in such scenarios since their implementation is rapid and inexpensive compared to the installation of ground relays or new base stations. Moreover, using UAVs offers a high level of coverage dynamicity which provides a better quality of service (QoS). In addition, one of the main advantages of using UAV compared to classical ground relays is the possibility of having a direct line of sight (LoS) with the other ground terminals. This fact offers better channel gain, lower power consumption, and longer battery life. The concept of using UAVs for wireless communications is currently a proven technology and has been tested and deployed in real case scenarios using LTE [13]. In [14], UAV-based communications were proposed as a potential solution to cope with spectrum congestion. Recent works [15]–[17] in the literature have been studying optimized ways to implement UAVs.

Currently, deploying UAV-assisted wireless networks faces multiple challenges such as maintaining efficient communication, reducing delays and, designing robust routing protocols [18]. However, the corresponding advantages are also multiple: extending coverage, enhancing reliability, and easy deployment especially in emergency situations [19]. Consequently, studying the corresponding performance in terms of spectral efficiency is important in order to evaluate their impacts once adopted as a part of wireless networks. In the literature, multiple works studied the placement of the UAVs that offers the maximum performance [16], [20]. The relaying can be employed using multiple techniques: i) the amplify-and-forward (AF), [21], in which the relay amplifies the received signal before broadcasting it to the destination, ii) decode-and-forward (DF), [22], where the relay decodes the message and then re-encodes it before retransmission, and iii) compress-and-forward (CF), [23], in which the relay compresses the received signal and forwards its estimate.

In the AF mode which is adopted in this paper, the relay, in addition to its power budget, is characterized by its amplification gain. This gain is either fixed in the case of partially-cooperative relaying or optimized in the case of fully-cooperative relaying. The partially-cooperative relaying represents a scenario where the amplification gain is fixed due to, for instance, the unavailability of the channel state information (CSI) or computational ''intelligence'' at the relay node. On the other hand, the fully-cooperation relaying represents a situation where the gain at the ''intelligent'' relay is adaptive with the CSI to enhance the achievable rate.

From another side, MIMO communications were proposed in order to increase the throughput/reliability by exploiting the spatial multiplexing/diversity [24], [25]. The fact of spreading the power over multiple antennas remarkably enhances the spectral efficiency even with only two antennas [26]. Multiple previous works studied relay-assisted MIMO systems [10], [27]. In the fully-cooperative MIMO relaying, the relay matrix amplification gain, or simply the relay matrix, needs to be optimized in order to achieve higher performances than the case of a fixed relay matrix [28]–[31].

In addition to relaying, the concept of cognitive radio (CR) is presented to enhance wireless communications as a solution to overcome the inefficient spectrum allocation [32]. In this concept, cognitive/secondary users (SU) share the spectrum of licensed/primary users (PU) without affecting the primary communication [33]–[35]. In the CR framework, the problem becomes more complex due to the additional constraints imposed by the license owners. Several studies have been proposed to devise practical solutions in the CR context. Perlaza *et al.* [36], Kang *et al.* [37], and Sboui *et al.* [38] and [39] have studied the MIMO CR power allocation problem. The relay-assisted CR systems were analyzed in [40]–[44]. Zhao *et al.* [40] studied a classical relay-assisted interweave CR system and established a trade-off between the rate and the successful communication probability. Li *et al.* [41] proposed a relay selection approach in cooperative CR systems. In [43] and [44], the power allocation for a relay and multi-relays CR MIMO was presented but with fixed gain, respectively.

The multi-access CR with a common receiver for the PU and SU was studied in [45]–[49]. This setting describes a primary base station that receives opportunistic SU transmissions which can be adopted by cellular operators to meet the need for two categories of users: (i) licensed users that benefit from reliable QoS, (ii) unlicensed users that share the spectrum to reach the closest BS and pay a certain cost for this service. Another implementation of spectrum sharing with a common receiver is the recent unlicensed long term evolution (LTE-U) where users can share unlicensed spectrum through a common access point or base station [50].

By combining the aforementioned key enabling technologies with the innovative UAVs, complex and important challenges have to be addressed. In this paper, we investigate the multi-access CR system using MIMO antennas for primary and secondary users supported by a UAV relay. The objective is to examine the maximum achievable rate of the cognitive user as well as the effect of the relay parameters on both primary and cognitive rates in the partially and fully-cooperative modes of the UAV relay. We propose an algorithm optimizing the relay amplification matrix in order to maximize both PU and SU rates. This framework is mainly motivated by cooperative communications between primary and cognitive networks. We focus on the case where both PU and SU are far from any base station and a UAV relay is employed to allow both users to communicate to the closest primary BS and then routing the information using the UAV as described in [51].

The received secondary message at the BS is then transferred to the secondary network via the backhaul connection between the both core networks given a certain cost as part of the cooperation between both networks. Hence, the corresponding secondary achievable rate and the impact of this cooperation on the PU need to be analyzed. The SU aims to maximize its rate, by allocating its power optimally among its antennas depending on the communication environment while considering the primary communication activity. On the other hand, PU optimizes its transmission without considering the existence of SUs. Such scenarios can be applied in different practical situations. For instance, in the context of public safety communication, where both PU and SU are located in a remote or damaged infrastructure area, a UAV comes to support the PU transmission but also

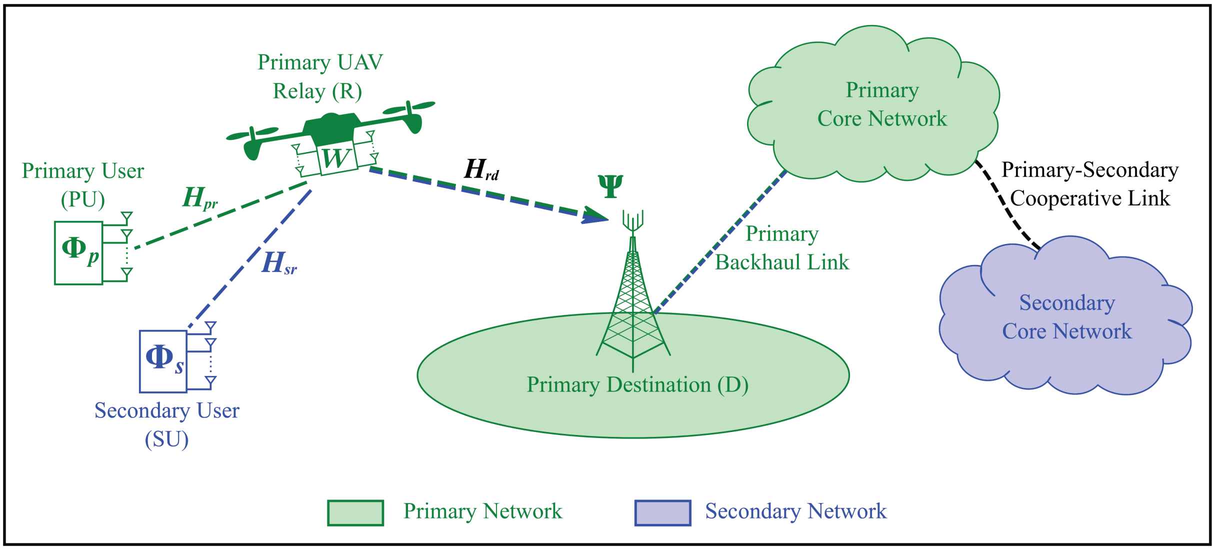

FIGURE 1. An uplink spectrum sharing communication in presence of a UAV relay.

allow the transfer of the secondary data whenever the primary communication QoS allows. Another scenario is the case where two users having different priority levels are aiming to exploit the limited power budget of the UAV relay to complete their transmission. Hence, the highest priority user, namely PU, will have the advantage to exploit the UAV resources first while the lowest priority user, SU, will try to exploit the remaining resources without harming the primary transmission.

In our setting, after a particular precoding at the PU transmitter based on a singular value decomposition (SVD), some free eigenmodes, i.e., parallel channels, are unused and thus can be freely exploited by the SU. In addition, the SU is allowed transmit through the PU used eigenmodes while respecting an interference threshold tolerated by the PU. That is, SU implements a space alignment approach and its signal is sent on both the free and the non-free eigenmodes [43]. The resulting signal is amplified and retransmitted to the destination where the primary signal is decoded first as it is expected to be the strongest one since the SU signal is always limited by the interference threshold imposed by the PU. Afterward, we adopt a successive interference cancellation (SIC) decoder [52] in order to decode the PU and the SU signals. In our analysis, we study the accuracy of the SIC decoder on the cognitive power allocation. We also present an alternate search algorithm that determines the optimal transmit power and relay matrix in the case of fully-cooperative relaying [53]. The main contributions of this work are as follows:

- Derive closed-form expressions of the optimal PU and SU transmit power levels for space alignment relay-assisted scenario;
- Analyze the accuracy of the SIC by presenting the optimal CR transmit power in the extreme cases: perfect and imperfect SIC;
- Determine the optimal transmit power level and relay matrix amplification gain using a alternate search algorithm in the fully-cooperative relaying case.
- Investigate the performance of the UAV relay and identify its advantages compared to the traditional ground relay.

The rest of this paper is organized as follows. In Section II, the system model is presented. Section III describes the proposed power allocation scheme when the relay matrix is fixed. In Section IV, the proposed algorithm that determines the optimal transmit power and relay matrix in the case of the fully-cooperative relay is presented. Numerical results are presented in Section V. Finally, the paper is concluded in Section VI.

II. SYSTEM MODEL

We consider an uplink multi-access communication scenario as depicted in Fig.1, where PU and SU are interested in transmitting their signals simultaneously to the closest primary BS called primary destination and denoted by D. The secondary message is first transferred to the primary core network and then to the secondary core network using a cooperative connection between the primary and secondary core networks. This type of cooperative connection is expected to be performed thanks to the emergence of network function visualization (NFV) and software-defined networks (SDN) concepts [54]. This service is part of cooperation between both networks were the SUs pay a roaming fee for being served by the primary network. This scenario is very relevant to public safety communication especially when the infrastructure of the secondary network is damaged.

We assume that the users are out of the range of D meaning that there is no direct link between the transmitters and the common receiver. A UAV relay, denoted by R, is implemented by the primary network to ensure the communication between the terminals by amplifying the received signal and forwarding it to the destination D. The PU, as a licensed node, freely exploits the channel while the SU, as an unlicensed node, is allowed to share the spectrum opportunistically and to access the channel under some constraints that maintain a certain QoS of the primary communication. Note that by having a lower priority with respect to the PU, the SU is opting for a "best effort" communication which means that the SU does not have constraints related to the minimal rate or the service outage.

A. CHANNEL MODEL

Each node is equipped with N antennas, and the channel gain matrices representing the links between the PU and R (PU-R), between SU and R (SU-R), and between R and D (R-D) are denoted by $\boldsymbol{H_{pr}}$, $\boldsymbol{H_{sr}}$, and $\boldsymbol{H_{rd}}$, respectively. In the case where the number of antennas at the receivers, denoted by N_r, and the transmitters, denoted by N_t, is different, we take $N = \min\{N_r, N_t\}$ [55]. Since the UAV relay is located at a relatively high altitude, all channel gains with the other nodes Q (Q $\in$ {PU, SU, D}) correspond to air-to-ground (A2G) channels including the path loss and fast fading effects [4]. They are expressed as follows:

$$\boldsymbol{H} = \frac{\tilde{\boldsymbol{H}}}{\sqrt{PL}}, \tag{1}$$

where $\tilde{\boldsymbol{H}}$ is the normalized channel gain and PL is the path loss effect between R and Q that are separated by a distance, denoted by d_Q, which corresponds to the Euclidean distance and is expressed as $d_Q = ||\boldsymbol{X}_R - \boldsymbol{X}_Q|| = \left((x_R - x)^2 + (y_R - y)^2 + (z_R - z)^2\right)^{\frac{1}{2}}$ where $\boldsymbol{X}_R$ and $\boldsymbol{X}_Q$ are the geographical coordinates of nodes R and Q, respectively, and $||.||$ is the 2-norm distance.

In the A2G channel, the LoS links between the flying UAV and the ground nodes are assumed to be available with a certain probability denoted by p^{LoS}. The average A2G free space path loss, PL, is given as follows [16]:

$$PL = p^{\mathrm{LoS}} PL^{\mathrm{LoS}} + (1 - p^{\mathrm{LoS}}) PL^{\mathrm{NLoS}}, \tag{2}$$

with

$$p^{\mathrm{LoS}} = \frac{1}{1 + \psi_1 \exp(-\psi_2[\theta - \phi])}, \tag{3}$$

where θ is the elevation angle between nodes R and Q in degree which depends on the distance d between R and Q, and ψ_1 and ψ_2 are constant values that depend on the environment. In (2), PL^{LoS} and PL^{NLoS} denote the LoS and NLoS free space path losses and are given in dB as:

$$PL^{\mathrm{LoS}} = 10\nu \log_{10}\left(\frac{4\pi f d}{C}\right) + L_{\mathrm{LoS}}, \tag{4}$$

$$PL^{\mathrm{NLoS}} = 10\nu \log_{10}\left(\frac{4\pi f d}{C}\right) + L_{\mathrm{NLoS}}, \tag{5}$$

where ν is the path loss exponent, f is the carrier frequency, C is the speed of light, and L_{LoS} and L_{NLoS} are the average additional losses to the free-space propagation losses for the LoS and NLoS links. Their values depend on the environment.

The fast-fading channel gain, $\tilde{\boldsymbol{H}}$ is modeled as a Rician fading channel composed of two components: a LoS component assumed to be constant and deterministic and a Rayleigh fading component representing the multipath reflection and is expressed as follows [11]:

$$\tilde{\boldsymbol{H}} = \sqrt{\frac{K}{K+1}} e^{i\phi} \tilde{\boldsymbol{H}}^{\mathrm{LoS}} + \sqrt{\frac{1}{K+1}} \tilde{\boldsymbol{H}}^{\mathrm{NLoS}}, \tag{6}$$

where K is the Rician factor, ϕ is the phase shift of the signal between the transmitting and receiving antennas, $\tilde{\boldsymbol{H}}^{\mathrm{LoS}}$ is a constant term and corresponds to the LoS component, and $\tilde{\boldsymbol{H}}^{\mathrm{NLoS}}$ corresponds to the NLoS fading component. The Rician factor K is selected such that $p^{\mathrm{LoS}} = \frac{K}{K+1}$.

B. SIGNAL MODEL

The transmission between the transmitters and the common receiver takes place during two time slots. In the first time slot, the PU and the SU terminals transmit simultaneously their signals to the relay where the complex received vector is given by:

$$\boldsymbol{y_R} = \boldsymbol{H_{pr}} \boldsymbol{\Phi_p} \boldsymbol{s_p} + \boldsymbol{H_{sr}} \boldsymbol{\Phi_s} \boldsymbol{s_s} + \boldsymbol{z_R}, \tag{7}$$

where $\boldsymbol{H_{pr}}$ and $\boldsymbol{H_{sr}}$ are assumed to be independent, $\boldsymbol{\Phi_p}$ and $\boldsymbol{\Phi_s}$ are the linear precoding matrices applied at the PU and SU, and $\boldsymbol{s_p}$ and $\boldsymbol{s_s}$ are independent and identically distributed (i.i.d.) complex Gaussian signals transmitted by PU and SU, respectively. For $i \in \{p, s\}$, we consider $\boldsymbol{P_i} = \mathbb{E}[\boldsymbol{s_i}\boldsymbol{s_i}^h]$ to be the covariance matrix of the vector $\boldsymbol{s_i}$, where $\mathbb{E}[\cdot]$ is the expectation over all channel realizations and $.^h$ designates the transpose conjugate operator. This covariance matrix is subject to a power constraint $Tr\ (\boldsymbol{\Phi_i} \boldsymbol{P_i} \boldsymbol{\Phi_i}^h) \leq P_{tot}$ where $Tr\ (\boldsymbol{A}) = \sum_j A(j,j)$ is the *trace* of the matrix $\boldsymbol{A}$, and P_{tot} is the total power budget considered, without loss of generality, to be the same for both users. Finally, $\boldsymbol{z_R}$ indicates a zero mean additive white Gaussian noise (AWGN) vector at the relay with a covariance matrix, $N_0 \boldsymbol{I_N}$ where $\boldsymbol{I_N}$ is the identity matrix with size N and N_0 is the noise variance expressed as $N_0 = k_B T B$ where k_B is the Boltzmann's constant, T is the temperature in Kelvin, and B is the total bandwidth. During the second time slot, the relay amplifies the signal $\boldsymbol{y_R}$ through an amplification gain matrix denoted by $\boldsymbol{W}$. Then, it retransmits the signal to the common destination D. The received signal $\boldsymbol{y_D}$ at the receiver D, is expressed as follows

$$\boldsymbol{y_D} = \boldsymbol{H_{pd}} \boldsymbol{\Phi_p} \boldsymbol{s_p} + \boldsymbol{H_{sd}} \boldsymbol{\Phi_s} \boldsymbol{s_s} + \boldsymbol{z}, \tag{8}$$

where $\boldsymbol{H_{pd}} = \boldsymbol{H_{rd}} \boldsymbol{W} \boldsymbol{H_{pr}}$, $\boldsymbol{H_{sd}} = \boldsymbol{H_{rd}} \boldsymbol{W} \boldsymbol{H_{sr}}$ and $\boldsymbol{z} = \boldsymbol{H_{rd}} \boldsymbol{W} \boldsymbol{z_R} + \boldsymbol{z_D}$, where $\boldsymbol{z_D}$ is an AWGN vector at the destination D with a covariance matrix, $N_0 \boldsymbol{I_N}$. Note that the covariance matrix of the equivalent noise $\boldsymbol{z}$, $\boldsymbol{Q_z}$, is written as follows:

$$\boldsymbol{Q_z} = N_0 \left(\boldsymbol{I_N} + \boldsymbol{H_{rd}} \boldsymbol{W} \boldsymbol{W}^h \boldsymbol{H_{rd}}^h\right). \tag{9}$$

Our the objective is to characterize the upper limits of the UAV-relayed CR performances. This upper limits of the performance cannot be obtained unless the CSI is perfect as we assumed. Hence, we assume that full channel state information (CSI) is available at the receiver and at the transmitters (i.e., PU-R, SU-R and R-D channel gains). We also assume that the destination provides a feedback about the CSI to the transmitters through the relay as part of the cooperation between both networks. In other words, the feedback about the CSI of the destination-UAV is performed first. Then, the CSI of the UAV-PU and UAV-SU links is performed. Afterwards, the UAV provides the transmitters with the resulting CSI's of the destination-PU and destination-SU links respectively.

Since the receiver at the destination is common to both transmitters, PU and SU signals are subject to mutual interference that may cause a significant deterioration to both primary and secondary performances. Therefore, in order to protect the licensed PU, we adopt an interference constraint [35] imposed by the PU to force the SU transmission to be below a certain interference threshold per receive antenna denoted by I_{th}. In fact, the interference threshold is a parameter that the primary network provides to the potential secondary users to share the spectrum, eventually for a certain financial reward paid by the secondary network. For this reason, communicating this parameter is performed either from the primary transmitter using broadcasting or from the UAV relay that belongs to the primary network and is aware of the interference threshold. In our case, this is more realistic since both users have common relay and receiver [56, Ch. 2].

III. SPACE ALIGNMENT PRECODING WITH FIXED RELAY MATRIX

This section introduces the proposed linear precoding and decoding matrices used, when the UAV relay has a fixed matrix gain, to maximize the SU rate while respecting the PU's QoS. The proposed scheme is also employed to exploit the space alignment technique, presented in [57], allowing the SU to transmit through the unused primary eigenmodes. Note that both users aim to maximize their achievable rates, and it is more convenient to maximize the sum-rate subject to the PU and SU constraints.

By having a perfect CSI of the PU-R and R-D links at the PU transmitter in addition to the knowledge of the fixed relay amplification matrix gain $\boldsymbol{W}$, the PU can optimally allocate the transmit power in order to maximize its achievable rate. Note that the knowledge of $\boldsymbol{W}$ at the transmitters is provided by the relay along with the CSI. By applying the SVD to $\boldsymbol{H_{pd}}$, the PU transmits through parallel channels characterized by their associated eigenmodes. Note that the SVD transformation does not entail any capacity loss since the precoding at the transmitter and the decoding at the receiver are both invertible as shown in [24]. The SVD of the matrix is denoted by $\boldsymbol{H_{pd}} = \boldsymbol{U}\boldsymbol{\Lambda}\boldsymbol{V}^h$ where $\boldsymbol{U}$ and $\boldsymbol{V}$ are two unitary matrices and $\boldsymbol{\Lambda}$ is a diagonal matrix that contains the ordered singular values of $\boldsymbol{H_{pd}}$ denoted by $\lambda_1 \geq \lambda_2 \geq \cdots \geq \lambda_N$.

A. PRIMARY USER ACHIEVABLE RATE

To transform the MIMO PU relay channel to N parallel channels, we employ the linear precoding $\boldsymbol{\Phi_p}$ at the PU node and the decoding $\boldsymbol{\Psi}$ at the destination, respectively, as follows:

$$\boldsymbol{\Phi_p} = \boldsymbol{V} \text{ and } \boldsymbol{\Psi} = \boldsymbol{U}. \tag{10}$$

Thus, the output received signal after decoding becomes:

$$\boldsymbol{r} = \boldsymbol{\Psi}^h \boldsymbol{y_D} = \boldsymbol{\Lambda} \boldsymbol{s_p} + \boldsymbol{U}^h \boldsymbol{H_{sd}} \boldsymbol{\Phi}_s \boldsymbol{s_s} + \tilde{z}, \tag{11}$$

where $\tilde{z} = \boldsymbol{U}^h z$ remains a zero mean AWGN with a covariance matrix $\boldsymbol{Q}_{\tilde{z}}$ given as follows:

$$\boldsymbol{Q}_{\tilde{z}} = N_0 \left(\boldsymbol{I_N} + \boldsymbol{U}^h \boldsymbol{H_{rd}} \boldsymbol{W} \boldsymbol{W}^h \boldsymbol{H_{rd}}^h \boldsymbol{U} \right). \tag{12}$$

In order to maximize its rate, the PU forces the interference caused by the vector $\boldsymbol{s} = \boldsymbol{U}^h \boldsymbol{H_{sd}} \boldsymbol{\Phi}_s \boldsymbol{s_s}$ to not exceed a fixed I_{th} per receive antenna, i.e., the covariance matrix of $\boldsymbol{s}$ denoted by $\boldsymbol{Q_s}$ satisfies the condition: $Q_s(j,j) \leq I_{th}$ for the j^{th} antenna, $j = 1, \ldots, N$. Therefore, the PU considers this eventual interference as a noise when maximizing its achievable rate R_p. This rate is considered to be the worst case scenario or a lower bound of the PU rate as the interference threshold, I_{th}, may not be reached by the SU. Hence, the optimal PU power and the rate lower bound are derived by solving the following optimization problem:

$$\underset{\boldsymbol{P_p}}{\text{maximize}}\ R_p = B \sum_{j=1}^{N} \log_2 \left(1 + \frac{P_p(j,j)\lambda_j^2}{I_{th} + Q_{\tilde{z}}(j,j)} \right) \tag{13}$$

$$\text{s.t. } Tr\ (\boldsymbol{P_p}) \leq P_{tot}, \tag{14}$$

$$Tr \left(\boldsymbol{H_p} \boldsymbol{P_p} \boldsymbol{H_p}^h + N_0 \boldsymbol{W} \boldsymbol{W}^h \right) \leq P_R, \tag{15}$$

where $\boldsymbol{H_p} = \boldsymbol{W} \boldsymbol{H_{pr}} \boldsymbol{\Phi_p}$. The constraint (15) indicates that the amplified signal power at the relay has to respect the total relay's power budget P_R. This optimization problem is convex with respect to $P_p(j,j)$'s as the objective function (13) is concave and the constraints are linear [58]. Hence, we apply the Lagrangian method to solve this problem. We first compute the Lagrangian function and then find its derivative with respect to each $P_p(j,j)$. The optimal power is given by:

$$P_p^*(j,j) = \left[\frac{B}{\mu_p + \eta_p \sum_{i=1}^{N} |H_p(j,i)|^2} - \frac{I_{th} + Q_{\tilde{z}}(j,j)}{\lambda_j{}^2} \right]^+, \quad \forall j = 1, \ldots, N, \tag{16}$$

where $[.]^+ = \max(0, .)$, μ_p and η_p are the Lagrange multipliers corresponding to the primary total power constraint and the relay total power constraint expressed in (14) and (15), respectively. From (16), when the channel gain is poor, i.e., λ_j's have small values, we note that the number of the used eigenmodes by PU can be less than the total number of antennas N. This case occurs when the optimal power allocated to the j^{th} antenna is zero (i.e., $P_p^*(j,j) = 0$). Consequently, the SU can freely exploit the unused eigenmodes. We denote by n ($0 \leq n < N$) the number of unused eigenmodes.

Note that the SU is aware of the value of n by computing the primary optimal power allocation which is possible since the primary CSI is provided by the relay. Then, we distinguish two sets of eigenmodes: $N-n$ eigenmodes used by the PU and n unused eigenmodes that can be freely exploited by the SU.

In order to remove the SU channel effect from the received signal at the destination, i.e., in (11), we choose $\boldsymbol{\Phi_s}$ as follows:

$$\boldsymbol{\Phi_s} = (\boldsymbol{H_{sd}})^{-1}\boldsymbol{U}. \tag{17}$$

The choice of the precoder matrix $\boldsymbol{\Phi_s}$ does not impact the system performance in our context as long as we are also optimizing the secondary transmit power vector $\boldsymbol{P_s}$. Indeed, since these two parameters belong to the same user, fixing one and optimizing the other or optimizing both of them simultaneously lead to the same result. Hence, $\boldsymbol{\Phi_s}$ is chosen such that the receiver can apply the same decoder $\boldsymbol{\Psi}$ and the mathematical analysis is simplified.

Without loss of generality, we assume that $\boldsymbol{H_{sd}}$ is invertible otherwise $(\boldsymbol{H_{sd}})^{-1}$ can be taken as the pseudo-inverse of $\boldsymbol{H_{sd}}$. Note that, since the SU is aware of the PU CSI, (i.e., $\boldsymbol{H_{pr}}$ and $\boldsymbol{H_{rd}}$), the unitary matrix $\boldsymbol{U}$ can be computed at the SU transmitter. As mentioned earlier, we assumed that there is a feedback through which the receiver can broadcast this information to the cognitive user. This is not a very benign assumption as feedback CSI is adopted in most wireless communication protocols. Consequently, the received signal is expressed as:

$$r_{D_j} = \begin{cases} \lambda_j s_{pj} + s_{sj} + \tilde{z}_j, & \forall j = 1, \ldots, N-n, \\ s_{sj} + \tilde{z}_j, & \forall j = N-n+1, \ldots, N. \end{cases} \tag{18}$$

Typically, the SU signal is always constrained by the interference threshold forced by the PU. Thus, in order to decode the SU signal, we propose to employ a SIC in order to cancel out the effect of the (strongest) signal, $\boldsymbol{s_p}$ from the received signal. Note that the SU signal, transmitted over the n free eigenmodes (FE), is only constrained by the total power constraints at the SU terminal and the relay.

B. SECONDARY USER ACHIEVABLE RATE

In this section, we investigate the achievable rate of SU using the proposed strategy described in Section III depending on the SIC performance. First, we derive the SU optimal power allocation assuming a perfect SIC (a genie SIC). Then, we investigate the gain in performance with an imperfect SIC (i.e., totally erroneous SIC). We introduce a parameter α $(0 \le \alpha \le 1)$ that corresponds to the probability of detecting the PU signal $\boldsymbol{s_p}$ correctly before applying the SIC. The achievable realistic scenarios obtained through a partial successful SIC are bounded by these two extreme cases: perfect SIC and imperfect SIC.

1) PERFECT SIC

In this case, we assume that the PU signal is always decoded perfectly, i.e., $\hat{s}_{p_j} = s_{p_j}, \forall j = 1, \ldots, N-n$, where $\hat{s}_{p_j}$ is the estimated PU signal at the jth receive antenna. Hence, the PU effect cancellation is performed correctly $(\alpha = 1)$ and, in this case, the output received signal after the SIC decoding, $\tilde{\boldsymbol{r}}$, is written as

$$\tilde{\boldsymbol{r}} = \boldsymbol{r} - \boldsymbol{\Lambda}\hat{\boldsymbol{s}}_{\boldsymbol{p}} = \boldsymbol{s_s} + \tilde{z}. \tag{19}$$

In fact, the proposed precoding scheme described in (17) has normalized the secondary channel. Consequently, the maximum achievable rate $R_s{}^{(\alpha=1)}$ is obtained by solving the following optimization problem:

$$\max_{\boldsymbol{P_s}} \; R_s{}^{(1)} = B\sum_{j=1}^{N}\log_2\left(1+\frac{P_s(j,j)}{Q_{\tilde{z}}(j,j)}\right) \tag{20}$$

$$\text{s.t. } Tr(\boldsymbol{\Phi_s}\boldsymbol{P_s}\boldsymbol{\Phi_s}{}^h) \le P_{tot}, \tag{21}$$

$$Tr\left(\boldsymbol{H_p}\boldsymbol{P}_{\boldsymbol{p}}^{*}\boldsymbol{H_p}{}^h + \boldsymbol{H_s}\boldsymbol{P_s}\boldsymbol{H_s}{}^h + N_0\boldsymbol{W}\boldsymbol{W}^h\right) \le P_R, \tag{22}$$

$$P_s(j,j) \le I_{th}, \quad \forall j = 1, \ldots, N-n, \tag{23}$$

where $\boldsymbol{P}_{\boldsymbol{p}}^{*}$ is the optimal PU power obtained after solving the optimization problem given in (13)-(15). This problem is also convex as the objective function is concave and the three constraints are linear. Note that the secondary precoding matrix in (17) is not unitary; thus, it should be included in the power budget constraint (21). Similarly to (15), when allocating its power, SU has to satisfy the relay power constraint (22) while considering the PU power obtained in (16). By using the invariance of the *trace* operator under cyclic permutations, the constraint (21) can be written as $Tr\ (\boldsymbol{\Phi_s}{}^h\boldsymbol{\Phi_s}\boldsymbol{P_s}) \le P_{tot}$. By defining the matrix $\boldsymbol{A_s} = \boldsymbol{\Phi_s}{}^h\boldsymbol{\Phi_s}$, (21) becomes $Tr\ (\boldsymbol{A_s}\boldsymbol{P_s}) \le P_{tot}$.

Since the constraint (23) is a peak constraint, we divide the problem into two subproblems with the same objective function but with constraints (21) and (22) for the first subproblem and with the constraint (23) in the second. Then, we take the minimum between the two solutions [59]. For the first subproblem, we, again, use the Lagrangian method [58] to find the optimal solution. For the second subproblem, it is clear that I_{th} is the optimal solution $\forall j = 1, \ldots, N-n$. Finally, the resulting power profile is given as follows:

$$P_s^*(j,j) = \begin{cases} \min\left\{\left[\dfrac{B}{\mu A_s(j,j)+\eta\sum_{i=1}^{N}|H_s(j,i)|^2} - Q_{\tilde{z}}(j,j)\right]^+, I_{th}\right\}, \\ \qquad\qquad \forall j = 1, \ldots, N-n, \\ \left[\dfrac{B}{\mu A_s(j,j)+\eta\sum_{i=1}^{N}|H_s(j,i)|^2} - Q_{\tilde{z}}(j,j)\right]^+, \\ \qquad\qquad \forall j = N-n+1, \ldots, N, \end{cases} \tag{24}$$

where μ and η are the Lagrange multipliers associated with the secondary power budget and the relay power constraints, respectively. Note that when the PU does not tolerate any interference, i.e., $I_{th} = 0$, the SU is still able to transmit using the FE and the corresponding rate is noted as the FE rate.

2) IMPERFECT SIC

In Section III-B.1, we considered the ideal case when capacity achieving codes are employed by the PU transmitter. Since the PU rate is smaller than the PU mutual information, arbitrary low decoding error probability is achievable. In this subsection, we assume that instead of using capacity achieving codes, PU employs more practical coding schemes and thus decoding errors are unavoidable no matter how small the PU rate is. To capture this setting, we have introduced the parameter α. In this case, we investigate the extreme scenario ($\alpha = 0$) when the receiver decodes the cognitive message after employing an imperfect SIC where the interference power at each antenna is equal to $\mathbb{E}\left[\left|\tilde{\lambda}_j\left(s_{p_j} - \hat{s}_{p_j}\right)\right|^2\right] = 2\ P_p^*(j,j)\lambda_j{}^2$. Then, the SU achievable rate is obtained by solving the following optimization problem:

$$\max_{\boldsymbol{P_s}} R_s{}^{(0)} = B\sum_{j=1}^{N-n}\log_2\left(1+\frac{P_s(j,j)}{Q_{\tilde{z}}(j,j)+2P_p^*(j,j)\lambda_j{}^2}\right)$$
$$+B\sum_{j=N-n+1}^{N}\log_2\left(1+\frac{P_s(j,j)}{Q_{\tilde{z}}(j,j)}\right) \tag{25}$$
$$\text{s.t. } Tr(\boldsymbol{A_s P_s}) \le P_{tot}, \tag{26}$$
$$Tr\left(\boldsymbol{H_p P_p^* H_p}^h + \boldsymbol{H_s P_s H_s}^h + N_0\boldsymbol{W}\boldsymbol{W}^h\right) \le P_R, \tag{27}$$
$$P_s(j,j) \le I_{th}, \quad \forall j = 1,\ldots,N-n. \tag{28}$$

This problem is also convex and the optimal power is computed similarly to the perfect SIC case by using the Lagrangian method, the optimal power is given by:

$$P_s^*(j,j) = \begin{cases} \min\left\{\left[\dfrac{B}{\mu A_s(j,j)+\eta\sum_{i=1}^{N}|H_s(j,i)|^2} \right.\right. \\ \qquad \left.\left. -\left(Q_{\tilde{z}}(j,j)+2P_p^*(j,j)\lambda_j{}^2\right)\right]^+, I_{th}\right\}, \\ \qquad \forall j = 1,\ldots,N-n, \\ \left[\dfrac{B}{\mu A_s(j,j)+\eta\sum_{i=1}^{N}|H_s(j,i)|^2} - Q_{\tilde{z}}(j,j)\right]^+, \\ \qquad \forall j = N-n+1,\ldots,N, \end{cases} \tag{29}$$

where μ and η are the Lagrange multipliers associated to constraints (26) and (27), respectively. We notice, here, that the optimal power depends on the primary power and eigenmodes meaning that the secondary is adapting its power continuously with the variation of the primary channel state.

IV. SPACE ALIGNMENT PRECODING WITH OPTIMIZED RELAY MATRIX

In the fully-cooperative setting, the UAV relay adapts its amplification gain matrix with respect to the primary CSI in order to further enhance the PU rate. This procedure is possible when the channel matrices $\boldsymbol{H_{pr}}$ and $\boldsymbol{H_{rd}}$ are perfectly known then, the relay amplification matrix gain $\boldsymbol{W}$ can be optimized.

Meanwhile, when there are FE, the elements of $\boldsymbol{W}$ corresponding to these FEs can be optimized to enhance the SU as well. First, we present the proposed method that optimizes $\boldsymbol{W}$ in order to maximize the PU rate. Then, we present the updated power allocation optimization at the SU transmitter.

A. PRIMARY USER ACHIEVABLE RATE

Recall that from (8), the received signal can be written as follows:

$$\boldsymbol{y_D} = \boldsymbol{H_{rd}WH_{pr}\Phi_p s_p} + \boldsymbol{H_{rd}WH_{sr}\Phi_s s_s}$$
$$+\boldsymbol{H_{rd}Wz_R} + \boldsymbol{z_D}, \tag{30}$$

On one hand, the SVD of the matrices $\boldsymbol{H_{rd}}$ and $\boldsymbol{H_{pr}}$ are, respectively, given by:

$$\boldsymbol{H}_{pr} = \boldsymbol{U}_{pr}\boldsymbol{\Lambda}_{pr}\boldsymbol{V}_{pr}^h \text{ and } \boldsymbol{H}_{rd} = \boldsymbol{U}_{rd}\boldsymbol{\Lambda}_{rd}\boldsymbol{V}_{rd}^h. \tag{31}$$

where $\boldsymbol{U}_{pr}, \boldsymbol{U}_{rd}, \boldsymbol{V}_{pr}$, and $\boldsymbol{V}_{rd}$ are unitary matrices and where $\boldsymbol{\Lambda}_{pr}$ and $\boldsymbol{\Lambda}_{rd}$ are diagonal matrices containing the singular values of $\boldsymbol{H}_{pr}$ and $\boldsymbol{H}_{rd}$, respectively. On the other hand, it was proven in [60] that, in order to optimize the rate, the optimal gain-matrix has the following structure:

$$\boldsymbol{W} = \boldsymbol{V}_{rd}\boldsymbol{\Lambda}_W\boldsymbol{U}_{pr}^h \tag{32}$$

where $\boldsymbol{\Lambda}_W$ is a diagonal matrix to be optimized.

In the sequel, we denote by $\lambda_{x,j}, j = 1,\cdots,N$, the diagonal values of the matrix $\boldsymbol{\Lambda}_x, x \in \{rd, W, pr\}$. Hence, the received signal can be expressed as follows:

$$\boldsymbol{y_D} = \boldsymbol{U}_{rd}\boldsymbol{\Lambda}_{rd}\boldsymbol{\Lambda}_W\boldsymbol{\Lambda}_{pr}\boldsymbol{V}_{pr}^h\boldsymbol{\Phi_p s_p}$$
$$+\boldsymbol{U}_{rd}\boldsymbol{\Lambda}_{rd}\boldsymbol{\Lambda}_W\boldsymbol{U}_{pr}^h\boldsymbol{H_{sr}\Phi_s s_s}$$
$$+\boldsymbol{U}_{rd}\boldsymbol{\Lambda}_{rd}\boldsymbol{\Lambda}_W\boldsymbol{U}_{pr}^h\boldsymbol{z_R} + \boldsymbol{z_D}. \tag{33}$$

For the PU precoding and decoding, we choose the matrices $\boldsymbol{\Phi_p}$ and $\boldsymbol{\Psi}$ as:

$$\boldsymbol{\Phi_p} = \boldsymbol{V}_{pr} \text{ and } \boldsymbol{\Psi} = \boldsymbol{U}_{rd}, \tag{34}$$

For the SU precoding, we choose the matrix $\boldsymbol{\Phi_s}$ as:

$$\boldsymbol{\Phi_s} = \boldsymbol{H}_{sr}^{-1}\boldsymbol{U}_{pr}. \tag{35}$$

Consequently, the decoded received signal can be express as follows:

$$\boldsymbol{r_D} = \boldsymbol{\Psi}^h\boldsymbol{y_D} = \boldsymbol{\Lambda}_{rd}\boldsymbol{\Lambda}_W\boldsymbol{\Lambda}_{pr}\boldsymbol{s_p} + \boldsymbol{\Lambda}_{rd}\boldsymbol{\Lambda}_W\boldsymbol{s_s}$$
$$+\boldsymbol{\Lambda}_{rd}\boldsymbol{\Lambda}_W\boldsymbol{U}_{pr}^h\boldsymbol{z_R} + \boldsymbol{U}_{rd}^h\boldsymbol{z_D}. \tag{36}$$

Note that the resulting noise has a covariance matrix given by:

$$\boldsymbol{Q} = N_0\left(\boldsymbol{I_N} + \boldsymbol{\Lambda}_{rd}\boldsymbol{\Lambda}_W\boldsymbol{\Lambda}_W^h\boldsymbol{\Lambda}_{rd}^h\right). \tag{37}$$

Similarly to (13), we formulate an optimization problem that maximizes the primary achievable rate considering the worst scenario when maximum interference reached by SU is I_{th} per each antenna $j = 1,\cdots,N$. However, in this case, the decision variables are the diagonal matrices $\boldsymbol{P_p}$ and $\boldsymbol{\Lambda}_W$ that contain the primary transmit power per PU antenna and the amplification gain per relay antenna, respectively.

The optimization problem is given as follows:

$$\max_{P_p, \Lambda_W} R_p = B \sum_{j=1}^{N} \log_2 \left(1 + \frac{\lambda_{rd,j}^2 \lambda_{W,j}^2 \lambda_{pr,j}^2 P_p(j,j)}{N_0 + (I_{th} + N_0)\lambda_{rd,j}^2 \lambda_{W,j}^2} \right) \tag{38}$$

$$\text{s.t.} \sum_{j=1}^{N} P_p(j,j) \leq P_{tot}, \tag{39}$$

$$\sum_{j=1}^{N} \lambda_{W,j}^2 (N_0 + \lambda_{pr,j}^2 P_p(j,j)) \leq P_R. \tag{40}$$

Note that this optimization problem is not convex since the objective function is not convex with respect to Λ_W. However, the objective function is strictly quasi-concave with respect to Λ_W [61] and concave with respect to the $P_p(j,j)$'s. In order to solve this problem, we use an alternate search algorithm that iterates between maximizing the objective function with respect to the $P_p(j,j)$'s and with respect to Λ_W till reaching the convergence. This method is based on the alternate convex search presented in [53]. Note that the results in [62] mentioned that in a strictly quasi-concave problem, any local solution is a global solution. Hence, in our alternate convex search algorithm, in the step where we maximize the objective function with respect to Λ_W for fixed $P_p(j,j)$'s, we only need to find any maxima, which would be unique and global.

In the rest of this part, we describe the corresponding two maximization steps: with respect to $P_p(j,j)$'s, then with respect to Λ_W, then we present our alternate search algorithm. Finally, from the results in [53], performing an alternate search leads to the optimal solution of the objective function.

1) MAXIMIZATION WITH RESPECT TO THE TRANSMIT POWERS

We propose a Lagrangian based approach to find a suboptimal solution of this non-convex optimization problem. The Lagrangian for the problem (38)-(40) is given by:

$$\begin{aligned} L(P(j,j), \lambda_{W,j}, \mu_p, \nu_p) &= B \sum_{j=1}^{N} \log_2 \left(1 + \frac{\lambda_{rd,j}^2 \lambda_{W,j}^2 \lambda_{pr,j}^2 P_p(j,j)}{N_0 + (I_{th} + N_0)\lambda_{rd,j}^2 \lambda_{W,j}^2} \right) \\ &\quad + \mu_p \left(\sum_{j=1}^{N} P_p(j,j) - P_{tot} \right) \\ &\quad + \nu_p \left(\sum_{j=1}^{N} \lambda_{W,j}^2 (N_0 + \lambda_{pr,j}^2 P_p(j,j)) - P_R \right), \end{aligned} \tag{41}$$

where μ_p and ν_p are the Lagrange multipliers corresponding to constraints (39) and (40), respectively. By deriving the Lagrangian with respect to $P(j,j)$ and equating it to zero, we find the optimal $P(j,j)$ of the problem (38) for fixed Λ_W which is given by:

$$P_p^*(j,j) = \left[\frac{B}{\mu_p + \nu_p \lambda_{W,j}^2 \lambda_{pr,j}^2} - \frac{N_0 + (I_{th} + N_0)\lambda_{rd,j}^2 \lambda_{W,j}^2}{\lambda_{rd,j}^2 \lambda_{W,j}^2 \lambda_{pr,j}^2} \right]^+. \tag{42}$$

2) MAXIMIZATION WITH RESPECT TO THE RELAY GAIN MATRIX

On the other hand, we can derive the Lagrangian with respect to $\lambda_{W,j}$ and equating it to zero to obtain the following polynomial equations:

$$\lambda_{W,j} = 0, \quad \text{or } A \times \lambda_{W,j}^4 + B \times \lambda_{W,j}^2 + C = 0, \tag{43}$$

where A, B, and C are non-negative constants and are given by (44), as shown at the bottom of this page. We can, then, compute the optimal $\lambda_{W,j}^*$ maximizing the Lagrangian for fixed $P_p(j,j)$ and ν_p. The solution is either zero or one of the roots of the bi-quadratic polynomial equation given in (43) which is easy to solve. As $\lambda_{W,j}$ is a non-negative real number, we eliminate all the corresponding complex and negative roots and the optimal solution of $\lambda_{W,j}$ given $P_p(j,j)$ and ν_p is expressed as follows:

$$\lambda_{W,j}^* = \begin{cases} \sqrt{\dfrac{-B + \sqrt{\Delta}}{2A}}, & \text{if } \dfrac{-B + \sqrt{\Delta}}{2A} > 0, \\ 0, & \text{otherwise} \end{cases} \tag{45}$$

where $\Delta = B^2 - 4AC$ is the discriminant of the bi-quadratic polynomial equation.

The existence of a unique solution for this bi-quadratic polynomial equation with $A > 0$ in the positive real space $\mathbb{R}^+$ means that the solution is unique and global [62].

3) ALTERNATE SEARCH ALGORITHM

An inter-dependence between $P_p(j,j)$ and $\lambda_{W,j}$ is clearly noticed from equations (42) and (45). Therefore, we propose to adopt an alternate search algorithm in order to achieve the optimal solution of the problem formulated in (38).

We start by initializing the values of the matrix Λ_W and the Lagrange multiplier ν_p. Then, we compute the corresponding primary transmit power levels $P_p(j,j), \forall j = 1, \cdots, N$ which generate the new diagonal values of Λ_W by solving the

$$\begin{aligned} A &= \lambda_{rd,j}^4 N_0^3 \nu_p + 2I_{th}\lambda_{rd,j}^4 N_0^2 \nu_p + I_{th}^2 \lambda_{rd,j}^4 N_0 \nu_p + 2\lambda_{pr,j}^2 \lambda_{rd,j}^4 N_0^2 \nu_p P_p(j,j) + 3I_{th}\lambda_{pr,j}^2 \lambda_{rd,j}^4 N_0 \nu_p P_p(j,j) \\ &\quad + I_{th}^2 \lambda_{pr,j}^2 \lambda_{rd,j}^4 \nu_p P_p(j,j) + \lambda_{pr,j}^4 \lambda_{rd,j}^4 N_0 \nu_p P_p(j,j)^2 + I_{th}\lambda_{pr,j}^4 \lambda_{rd,j}^4 \nu_p P_p(j,j)^2, \\ B &= 2\lambda_{rd,j}^2 N_0^3 \nu_p + 2I_{th}\lambda_{rd,j}^2 N_0^2 \nu_p + 3\lambda_{pr,j}^2 \lambda_{rd,j}^2 N_0^2 \nu_p P_p(j,j) + 2I_{th}\lambda_{pr,j}^2 \lambda_{rd,j}^2 N_0 \nu_p P_p(j,j) \\ &\quad + \lambda_{pr,j}^4 \lambda_{rd,j}^2 N_0 \nu_p P_p(j,j)^2, \\ C &= B\lambda_{pr,j}^2 \lambda_{rd,j}^2 N_0 P_p(j,j) + N_0^3 \nu_p + \lambda_{pr,j}^2 N_0^2 \nu_p P_p(j,j) \end{aligned} \tag{44}$$

equations in (43) for a given ν_p. Note that the corresponding Lagrange multiplier μ_p can be determined using the primary peak power constraint given in (39). Afterward, we apply a backtracking line search in order to update the value of ν_p based on the Armijo-Goldstein condition [63]. Then, we recompute the new power levels and repeat this procedure until reaching convergence. Convergence is reached when the achievable rate remains constant after several numbers of iterations.

In **Algorithm 1**, we provide a detailed description of the alternate search algorithm applied to the primary optimization problem.

Algorithm 1 Alternate Search Algorithm for Primary User Rate Maximization

1: $t = 0$.
2: Initialize $\nu_p^{(t)}$ and $\lambda_{W,j}^{(t)}$, $j = 1, \cdots, N$.
3: Compute $P_p^{(t)}(j,j)$ corresponding to $\nu_p^{(t)}$ and $\lambda_{W,j}^{(t)}$ using (42).
4: Find the initial primary achievable rate $R_p^{(t)}$ using (38).
5: **repeat**
6: $\quad t \leftarrow t+1$.
7: $\quad$ Find the t^{th} values of $\lambda_{W,j}^{(t)}$, $j = 1, \cdots, N$ with respect to $P_p^{(t-1)}(j,j)$ and $\nu_p^{(t-1)}$ as it is given in (45).
8: $\quad$ Compute the corresponding $P_p^{(t)}(j,j)$.
9: $\quad$ Find $R_p^{(t)}$.
10: $\quad$ Update $\nu_p^{(t)}$ using a backtracking line search method.
11: **until** $|R_p^{(t)} - R_p^{(t-1)}|^2 \leq \epsilon$ where $\epsilon > 0$.
12: The optimal solution of the optimization problem formulated in (39) is $P_p^{(t)}(j,j)$ and $\lambda_{W,j}^{(t)}$, $\forall j = 1, \cdots, N$.

B. SECONDARY USER ACHIEVABLE RATE

After determining the optimal $\boldsymbol{P_p}$ and $\boldsymbol{W}$ that maximize the PU rate, the SU needs to maximize its rate by optimizing its transmit power levels while considering free and non-free eigenmodes.

Depending on the status of each primary eigenmode, the cooperative relay tries to enhance the SU rate by adjusting the related amplification gain in case it corresponds to the FE. Using (36), we derive the SU achievable rate expression for the perfect SIC scenario[1] as well as the corresponding optimization problem that is given as follows

$$\max_{\boldsymbol{P_s}, \tilde{\boldsymbol{\Lambda}}_W} R_s = B \sum_{j=1}^{N-n} \log_2 \left(1 + \frac{\lambda_{rd,j}^2 {\lambda_{W,j}^*}^2 P_s(j,j)}{N_0 \left(1 + \lambda_{rd,j}^2 (\lambda_{W,j}^*)^2\right)}\right) + B \sum_{j=N-n+1}^{N} \log_2 \left(1 + \frac{\lambda_{rd,j}^2 \lambda_{W,j}^2 P_s(j,j)}{N_0 \left(1 + \lambda_{rd,j}^2 \lambda_{W,j}^2\right)}\right) \tag{46}$$

$$\text{s.t.} \ \bullet\, Tr(\boldsymbol{A_s P_s}) \leq P_{tot}, \tag{47}$$

$$\bullet \sum_{j=1}^{N-n} {\lambda_{W,j}^*}^2 (N_0 + P_s(j,j) + \lambda_{pr,j}^2 P_p^*(j,j)) \tag{48}$$

$$+ \sum_{j=N-n+1}^{N} \lambda_{W,j}^2 (N_0 + P_s(j,j) + \lambda_{pr,j}^2 P_p^*(j,j)) \leq P_R,$$

$$\bullet \lambda_{rd,j}^2 (\lambda_{W,j}^*)^2 P_s(j,j) \leq I_{th}, \quad \forall j = 1, \ldots, N-n. \tag{49}$$

where $\tilde{\boldsymbol{\Lambda}}_W = [\lambda_{W,N-n+1}, \cdots, \lambda_{W,N}]$ is the vector containing the n diagonal elements $\lambda_{W,j}$ associated to the n primary FEs to be optimized in order to improve the SU achievable rate. Hence, if the PU is transmitting over all its eigenmodes then, $\tilde{\boldsymbol{\Lambda}}_W$ is an empty vector. The problem could be solved following the same approach employed to solve the PU problem in Section IV-A, while only considering the amplification gain associated to the FEs. The optimal SU power levels of (46) for a fixed $\tilde{\boldsymbol{\Lambda}}_W$ is given as follows:

$$P_s^*(j,j) = \begin{cases} \min\left\{\left[\dfrac{B}{\mu_s A_s(j,j) + \eta_s {\lambda_{W,j}^*}^2} - \dfrac{N_0\left(1 + \lambda_{rd,j}^2 {\lambda_{W,j}^*}^2\right)}{\lambda_{rd,j}^2 {\lambda_{W,j}^*}^2}\right]^+, \dfrac{I_{th}}{\lambda_{rd,j}^2 {\lambda_{W,j}^*}^2}\right\}, & \forall j = 1, \ldots, N-n, \\ \left[\dfrac{B}{\mu_s A_s(j,j) + \eta_s \lambda_{W,j}^2} - \dfrac{N_0\left(1 + \lambda_{rd,j}^2 \lambda_{W,j}^2\right)}{\lambda_{rd,j}^2 \lambda_{W,j}^2}\right]^+, & \forall j = N-n+1, \ldots, N, \end{cases} \tag{50}$$

where μ_s and η_s are the Lagrange multipliers associated to the peak and the relay power constraints, respectively.

Hence, we presented in this Section the optimal power allocation of both the PU and the SU when the UAV relay matrix is optimized. Intuitively, this optimization gives priority the PU since it will result in less free eigenmodes that the SU can exploit. In the next Section, we will investigate numerically the results of the optimized relay matrix cases versus the fixed relay.

V. NUMERICAL RESULTS

In this section, we evaluate our results for terminals with 4 antennas communicating to the UAV relay with 200 kHz of bandwidth. The UAV amplifies and forwards both PU and SU messages to the primary base station D. We present the variation of the average sum rate of primary and secondary users with the different parameters of the problem such as the power budget at the transmitters, the relay power budget, the relay gin matrix, and the relay altitude. We also highlight the sensitivity of our results to the imperfect CSI and the imperfect SIC. We also evaluate the complexity using the running time needed to reach the solution. We model the fading channel as a Rice fading channel where $\phi = \pi/4$, and hence $e^{i\phi} = \frac{1}{\sqrt{2}}(1+i)$. Also, we assume that $\boldsymbol{H_{LOS}}$ is

[1]The case of imperfect SIC follows a similar approach but with different objective function as shown in Section III.

TABLE 1. Simulation parameters.

Parameter	Value	Parameter	Value
LoS addi. path loss, L_{LoS} (dB)	1	Path loss exponent, ν	2
NLoS addi. path loss, L_{NLoS} (dB)	10	Bandwidth, B (kHz)	200
LoS probability parameter, ψ_1	9.6	LoS probability parameter, ψ_2	0.28
Number of antennas, N	4	Noise power, N_0/B (dBm/Hz)	-174

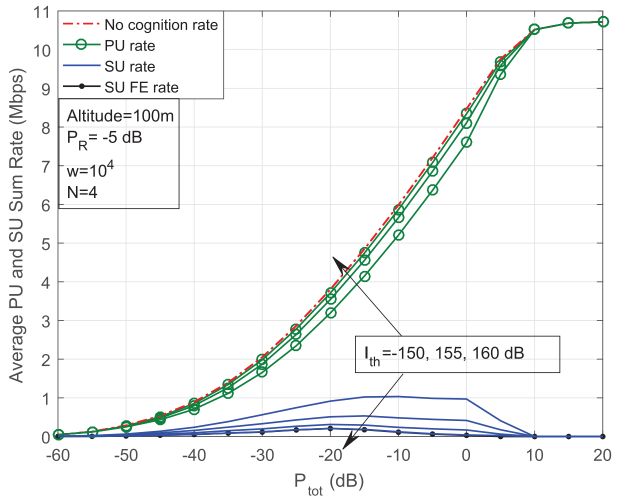

(a)

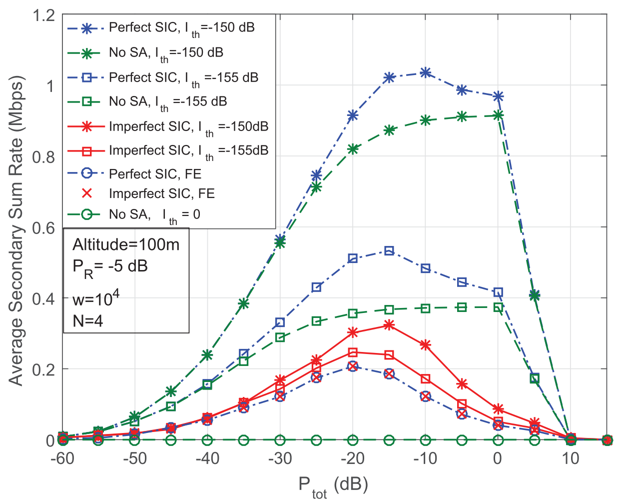

(b)

FIGURE 2. PU and SU rates versus P_{tot}. (a) Perfect SIC ($\alpha = 0$). (b) Imperfect SIC ($\alpha = 1$) and No SA.

given by $\boldsymbol{H}_{LOS} = \boldsymbol{I}_N$, and the $\boldsymbol{H}_{NLOS}$ is following a Rayleigh fading. The simulation parameters are given in Table 1 and the rates are expressed in Megabits per second (Mbps).

A. FIXED RELAY MATRIX NUMERICAL RESULTS

For simplicity, we assume that, in the fixed W case, the relay's amplification matrix is diagonal and is given by: $\boldsymbol{W} = w \times \boldsymbol{I}_N$ where w is a positive scalar. However, without loss of generality, the proposed scheme can be applied to any fixed relay matrix.

In Figure 2.a, we plot the PU and the SU achievable rates as a function of P_{tot} for $P_R = -5$ dB and $w = 10^4$ with perfect SIC ($\alpha = 0$). To measure the performance of the proposed system, we plot the rate limits when $I_{th} = 0$ which gives the upper bound of the PU rate: "no cognition rate" and the lower bound of the SU rate: "free eigenmodes (FE) rate", i.e., there is no tolerated interference from the PU. We show that the space alignment technique allows the SU to achieve a rate up to 0.2 Mbps when using only the FEs. However, this rate becomes zero when P_{tot} exceeds 15 dB since, in this case, the PU is using all the eigenmodes. Then, depending on the tolerated interference threshold, I_{th}, the SU rate is enhanced in the mid-range of P_{tot} since the power constraint (21) becomes inactive. Note that the PU rate slightly decreases with I_{th} which is acceptable since the PU tolerated this interference threshold. At high values of P_{tot}, the PU rate saturates at a particular value that depends mainly on the relay's power. That is, even if the PU has high power, the relay's power limits the received signal at the destination.

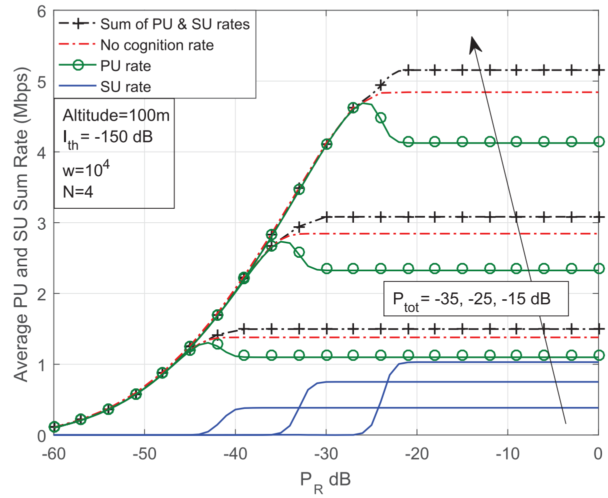

FIGURE 3. PU and SU rates with perfect SIC versus P_R.

In Figure 2.b, the SU rates with perfect and imperfect SIC are presented for $P_R = -5$ dB to quantify the rate loss when $\alpha = 1$. We notice that the rate loss increases with I_{th}. However, all imperfect SIC rates ensure rates higher than the SU FE rate. In addition, we compare Fig. 2.b, in, our algorithm with the classical underlay CR framework in which the SU transmits below the interference thresholds for each antenna that we denote by "No SA" for no space alignment. We show that our algorithm presents 10% and 20% sum rate enhancement for $I_{th} = -150$ and -155 dB, respectively. In addition, in the case where the PU does not allow any interference, i.e., $I_{th} \to 0$, our algorithm allow the SU to have a rate of 0.2 Mbps due to the FEs, whereas the No SA present a sum rate equal to zero.

Figure 3 shows the effect of the relay's power, P_R, on the PU and SU rates. First, we notice that even without cognition, the PU rates stagnate at high values of P_R since the power budget P_{tot} is exceeded by the relay's power level. In the case of cognition, for fixed $I_{th} = -150$ dB and when P_R is low, the cognitive rate increases from zero to a stagnation

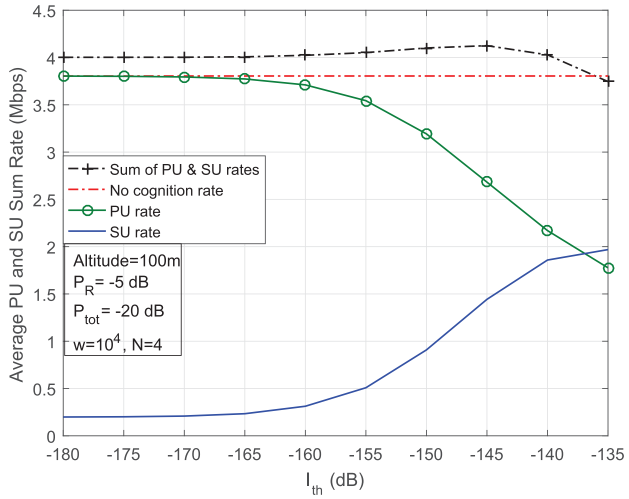

FIGURE 4. PU and SU rates with perfect SIC versus I_{peak}.

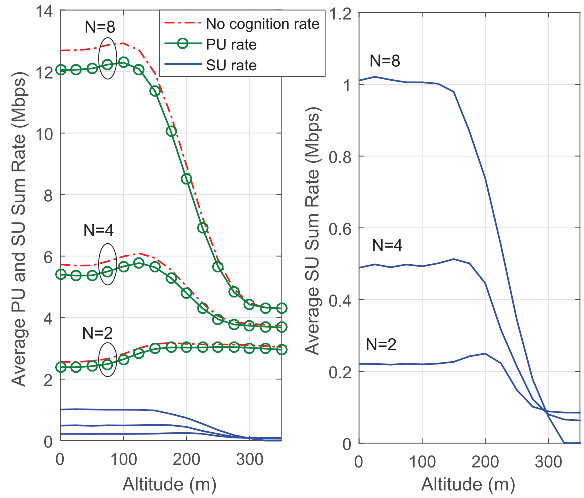

FIGURE 5. PU and SU rates versus the altitude of the UAV relay with $P_{tot} = -10$ dB, $w = 10^4$, $P_R = -5$ dB and $I_{th} = -155$ dB.

level (around 1 Mbps for $P_{tot} = -15$ dB) whereas, the PU rate increases at low values of P_R then, after a slight decrease, it stagnates at a value that is lower than the no cognition rate. In addition, we show that the sum rate of the PU and the SU is higher than the no cognition rate by 0.2-0.5 Mbps. Hence, the cognition enhances the spectrum efficiency and allows to have higher sum data rate than when only one user is using the spectrum.

Figure 4 shows that as I_{th} increases, the PU rate is gradually decreasing from 3.8 Mbps, i.e.,the no cognition rate, to 1.8 Mbps when $I_{th} = -135$ dB due to the tolerated interference. Meanwhile, the SU rate stagnates at around 0.2 Mbps for $I_{th} \leq -160$ dB then increases and reach 2 Mbps for $I_{th} = -135$. We also note from Fig. 4, that the sum rate is higher than the no cognition rate by $0.2 - 0.3$ Mbps and that it reaches a maximum $I_{th} = -145$ then decreases again. This observation can be explained by the fact that at low I_{th}, the PU rate is only limited by the relay power constraint and as I_{th} increases the PU rate increases and the SU rate increases. However, at high I_{th} values, the decrease of the PU rate is higher than the SU increase which reduced the sum rate as $I_{th} \geq -145$. Hence, the interference threshold I_{th} is considered as an envelope of the SU and PU rates at low and high values, respectively.

In Figure 5, we highlight the effect of the UAV altitude on both PU and SU rates for $N = 2, 4$ and 8. We show that when the altitude increases from the ground level to $100-150$m, the PU rate increases gradually as the LoS link is enhanced. For instance, for $N = 4$ from the PU rate increases from 5.4 Mbps to 5.8 Mbps between the ground and 125m. Beyond these altitudes, the PU rate starts to decrease, due to the path loss effect related to the increasing distance between the UAV and the PU. For instance for $N = 8$, the rate decreases from 12.3 Mbps to 4.3 Mbps between 100m and 350m whereas for $N = 2$, the PU rate slightly decreases from 3 Mbps to 2.9 Mbps between 150m and 350m. Hence, by observing the altitude effect on the spatial multiplexing in MIMO, we find that for a low number of antennas, e.g., 2 antennas, the altitude increases the link quality even at high altitudes. However, for 8 antennas the spatial multiplexing is reduced remarkably at high altitudes. From another side, the SU rate slightly increase at low altitudes: till 200m, 150m, and 100m for $N = 2, 4$ and 8. Then the SU rates decrease and reach the same rate equal to 0.075 Mbps at 300m. Hence, there are optimal altitudes that maximize both rates as shown in [16] depending on the number of antennas, which are, in our simulations around 200m, 150m, and 100m for $N = 2, 4$ and 8.

In Figure 6, we highlight the effect of the relay amplification matrix gain $\boldsymbol{W}$ on PU and SU rates for different values of P_R. Recall that, in our numerical results, we chose $\boldsymbol{W} = w \times \boldsymbol{I}_N$, which is not necessarily the optimal choice but is a simple one to quantify the effect of this matrix on the system performance. We notice that, even with no cognition, the rate reaches its maximum for a particular value of w before decreasing to zero as w increases. The reason behind this rate shape is that increasing w enhances the power as the relay power constraint is not reached. When reached, i.e., the values of w are large, the terminal power level should be small to respect the constraint and as w increases further, the power should be near zero. In the CR framework, the shape of the rate is similar but lower than the no cognition rate. The optimal w giving the maximum rate is different for PU and SU and can favor one over the other as shown in Figure 6 (a), (b) and (c). However, we notice that the w that maximizes the SU is almost the same $w = 2500$ regardless of the value of P_R which is not the case for the PU rate. For instance, the optimal PU w is 15000, 22500, and 32500 for $P_R = -10, -5$, and 0 dB, respectively.

B. OPTIMIZED RELAY MATRIX NUMERICAL RESULTS

In Figure 7, the PU and SU rates are plotted as a function of P_{tot} with full relay cooperation. We notice a higher PU rates

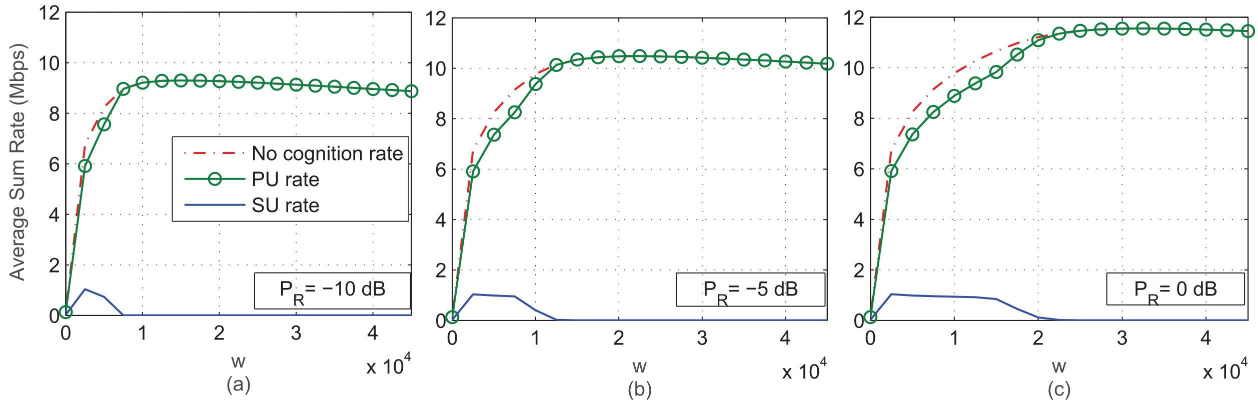

FIGURE 6. PU and SU rates with perfect SIC versus w with $P_{tot} = 5$ dB, $I_{th} = -150$ dB $N = 4$, and altitude of 100m.

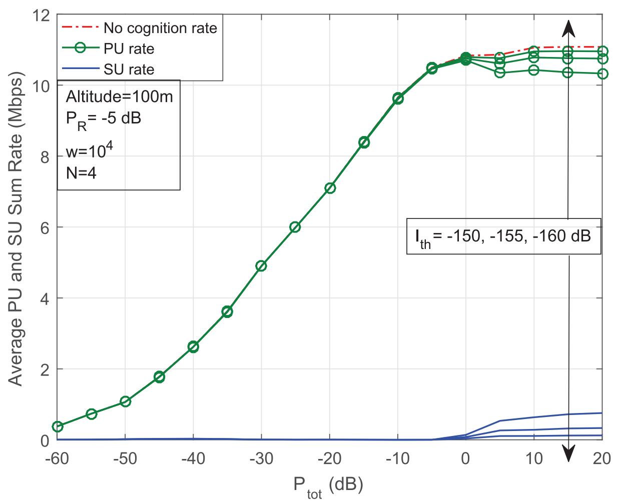

FIGURE 7. PU and SU rates versus P_{tot} with optimized W.

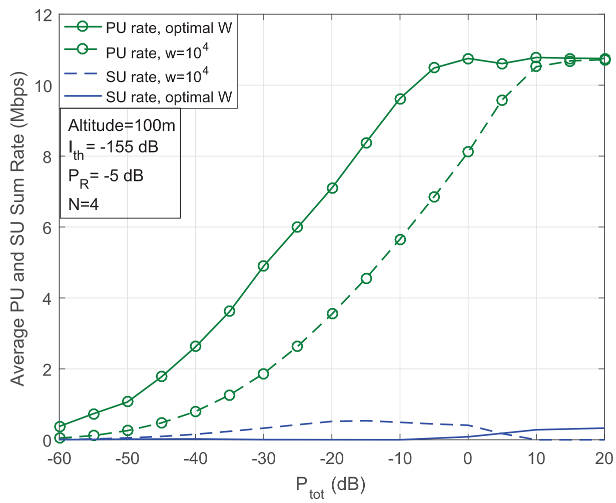

FIGURE 8. Comparison between the fixed and optimized W cases: the PU and SU rates as a function of P_{tot}.

versus a zero SU rate when $P_{tot} \leq -5$ dB. For instance, after the optimization of W, the PU rate reaches 5 Mbps instead of 2 Mbps at $P_{tot} \leq -30$. When $P_{tot} \geq -5$ dB, we show that the PU rate is slightly decreasing and the SU starts to increase. For instance, for $I_{th} = -150$ dB and $P_{tot} \geq 10$ dB, the PU decreases by 0.63 Mbps which represents 6.5% of the no cognition rate, whereas the SU rate reaches 0.63 Mbps. Consequently, the procedure of optimizing W for the PU allows to reach high PU rates and prevents the SU of transmitting except when there is an interference threshold and when $P_{tot} \geq -5$ dB.

In Figure 8, we perform a comparison of the PU and the SU rates using either optimized or fixed W (i.e., $\boldsymbol{W} = w \times I_N$ and $w = 10^4$). We show that, at low values of P_{tot}, optimizing $\boldsymbol{W}$ leads to a remarkable enhancement of the PU rate that reaches the non-cognition rate considered as the rate upper bound. This is essentially caused by the fact that the procedure of optimizing $\boldsymbol{W}$, described in **Algorithm 1** involves an optimization of the transmit power levels as well. This leads to a lower number of FEs and a reduced influence of I_{th}. The *PU* rate is enhanced by 277%, 185%, and 127% for $P_{tot} = -45, -35$ and -25 dB, respectively. Moreover, at low values of P_{tot} (≤ 5 dB), when $\boldsymbol{W}$ is optimized for the PU, the SU rate is lower than the fixed amplification gain case. For $P_{tot} \geq 5$ dB, the SU rate decreases to zero at high P_{tot} values whereas for the optimized $\boldsymbol{W}$, it reaches high values (about 0.2 Mbps in this case). This shows, again, that optimizing $\boldsymbol{W}$ in our proposed scheme reduces remarkably the number of FEs and hence, presents a trade-off between increasing the PU rate by optimizing $\boldsymbol{W}$ or the SU rate for a fixed $\boldsymbol{W}$. Note that, at high values of P_{tot}, the SU rate is close to zero due the fact that the FEs are very limited. Consequently, the power expression is mostly given by the first part of (50) which includes the relay matrix values $\lambda^*_{W,j}$ already optimized to the PU.

In Figure 9, we compare between the optimized and fixed $\boldsymbol{W}$ rate as function of P_R when $P_{tot} = -25$ dB. As it can be seen in Fig. 9, the PU rate enhancement due to $\boldsymbol{W}$ optimization is relatively small, i.e., 0.1 to 0.5 Mbps when $P_R \leq -35$ dB due to the limitation of the relay power.

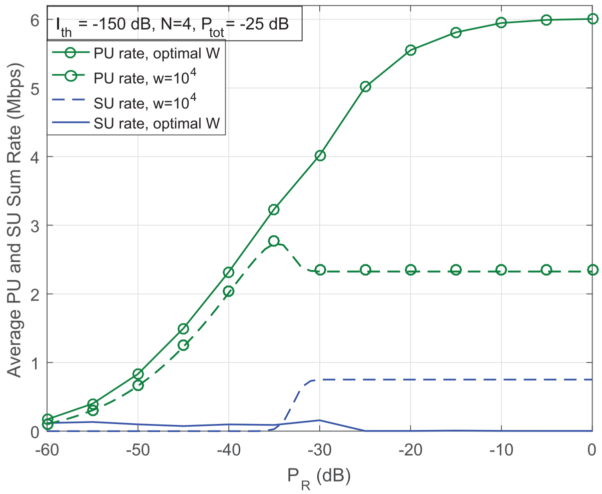

FIGURE 9. Comparison between fixed and optimized W: the PU and SU rates as a function of P_R.

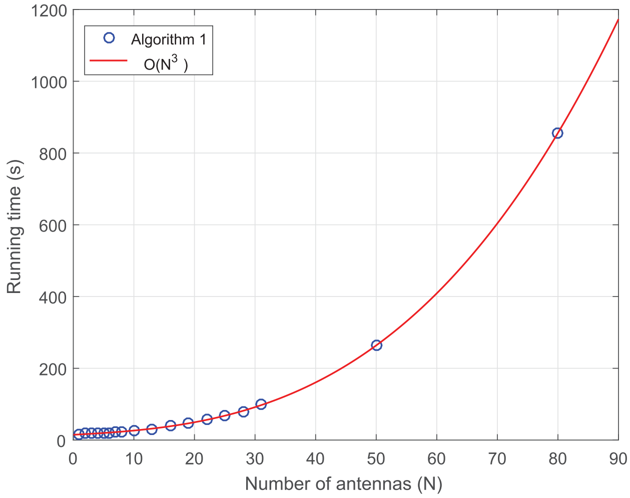

FIGURE 10. Running time of Algorithm 1 versus the number of antennas N.

However, this enhancement is remarkable when $P_R \geq -35$ as the PU rate goes from 2.35 Mbps to 4 Mbps and 6 Mbps for $P_R \geq -30$ dB and -5 dB, respectively. This observation reflects the importance of optimizing the relay matrix in order to achieve better performances with the available transmit and relay power budgets. In addition, we notice that, at this low relay power level ($P_R \leq -35$ dB), the SU rate using optimized $\mathbf{W}$ is higher than the one with fixed $\mathbf{W}$. However, as P_R increases, the SU rate with optimized $\mathbf{W}$ decreases till reaching zero. In fact, when $\mathbf{W}$ is optimized, increasing P_R, with fixed P_{tot}, will result in exploiting all the eigenvalues at the PU causing the SU to have very limited data rate.

In order to analyze the complexity of **Algorithm 1**, we plot, Fig. 10, the corresponding running time in seconds for 10^3 realizations as a function of the number of antennas N. We run our algorithm on workstation with 2 processors (Intel 2.67 GHz) on Windows. We perform a curve fitting of the obtained results and we show that **Algorithm 1** has a complexity corresponding to $O(N^3)$.

VI. CONCLUSION

In this paper, we investigated the achievable rate of a 5G scenario where a UAV relay is extending the wireless network and is serving both primary and secondary users in a cognitive radio framework. This work is a joint combination of multiple key enablers for 5G communi reflects the expected 5G scenarios that may cover cellular and public safety communications. We proposed a particular linear precoding scheme based on the space alignment strategy. By adopting this strategy, we computed the optimal power allocation for the cognitive user under power, interference, and relay's power constraints. We also derived the expressions of the optimal transmit power levels in different settings (perfect and imperfect successive interference cancellation) in order to provide upper and lower bounds of the cognitive rate. We also analyzed a fully-cooperative relaying scheme in which we optimized the UAV relay gain matrix and the transmit power levels through an alternate search algorithm. In our numerical results, we showed that our scheme ensured a non-zero cognitive rate up to a certain power budget. We presented the effect of the UAV altitude on both primary and secondary rates and found that there is an optimal altitude that maximizes both rates. Also, when the relay matrix gain is optimized to maximize the primary rate, we showed that the corresponding rate enhancement is about two to three folds. We also highlighted that the secondary rate presented some gains but only at high power regime. In summary, UAV relaying, in the CR context, allows the secondary user to communicate with an acceptable rate without degrading the primary communication. In addition, the achievable secondary rate is at its maximum when the UAV altitude is relatively at low altitude and adopting a fixed relay matrix gain. Finally, as the number of antennas increases the relative degradation of spatial multiplexing due to high altitudes increase.

REFERENCES

[1] L. Sboui, H. Ghazzai, Z. Rezki, and M.-S. Alouini, "On the throughput of cognitive radio MIMO systems assisted with UAV relays," in *Proc. Int. Wireless Commun. Mobile Comput. Conf. (IWCMC)*, Valencia, Spain, 2017.
[2] J. G. Andrews *et al.*, "What will 5G be?" *IEEE J. Sel. Areas Commun.*, vol. 32, no. 6, pp. 1065–1082, Jun. 2014.
[3] M. Peng, Y. Li, Z. Zhao, and C. Wang, "System architecture and key technologies for 5G heterogeneous cloud radio access networks," *IEEE Netw.*, vol. 29, no. 2, pp. 6–14, Mar./Apr. 2015.
[4] S. Chandrasekharan *et al.*, "Designing and implementing future aerial communication networks," *IEEE Commun. Mag.*, vol. 54, no. 5, pp. 26–34, May 2016.
[5] A. F. B. Hanscom and M. A. Bedford, "Unmanned aircraft system (UAS) service demand 2015-2035: Literature review & projections of future usage," U.S. Dept. Transp., Washington, DC, USA, Apr. 2015.
[6] M. Gharibi, R. Boutaba, and S. L. Waslander, "Internet of drones," *IEEE Access*, vol. 4, pp. 1148–1162, 2016.
[7] H. Satō, "Information transmission through a channel with relay," Aloha Syst., Univ. Hawaii, Honolulu, HI, USA, Tech. Rep. B76-7, Mar. 1976.
[8] T. M. Cover and A. A. El Gamal, "Capacity theorems for the relay channel," *IEEE Trans. Inf. Theory*, vol. 25, no. 5, pp. 572–584, Sep. 1979.
[9] C. Song, K.-J. Lee, and I. Lee, "MMSE-based MIMO cooperative relaying systems: Closed-form designs and outage behavior," *IEEE J. Sel. Areas Commun.*, vol. 30, no. 8, pp. 1390–1401, Sep. 2012.

[10] T. Luan, F. Gao, X.-D. Zhang, J. C. F. Li, and M. Lei, "Robust beamforming for relay-aided multiuser MIMO cognitive radio networks," in *Proc. IEEE Wireless Commun. Netw. Conf. (WCNC)*, Shanghai, China, Apr. 2013, pp. 2473–2477.

[11] A. Merwaday and I. Guvenc, "UAV assisted heterogeneous networks for public safety communications," in *Proc. IEEE Wireless Commun. Netw. Conf. Workshops (WCNCW)*, New Orleans, LA, USA, Mar. 2015, pp. 329–334.

[12] Y. Zeng, R. Zhang, and T. J. Lim, "Wireless communications with unmanned aerial vehicles: Opportunities and challenges," *IEEE Commun. Mag.*, vol. 54, no. 5, pp. 36–42, May 2016.

[13] M. Hainzl, "Integrating UAVs into public safety LTE networks," MSEMBC Prog., New Jersey Inst. Technol., Newark, NJ, USA, Tech. Rep. IS614-851, 2013.

[14] Y. Saleem, M. H. Rehmani, and S. Zeadally, "Integration of cognitive radio technology with unmanned aerial vehicles: Issues, opportunities, and future research challenges," *J. Netw. Comput. Appl.*, vol. 50, pp. 15–31, Apr. 2015.

[15] S. Rohde and C. Wietfeld, "Interference aware positioning of aerial relays for cell overload and outage compensation," in *Proc. IEEE Veh. Technol. Conf. (VTC Fall)*, Quebec City, QC, Canada, Sep. 2012, pp. 1–5.

[16] M. Mozaffari, W. Saad, M. Bennis, and M. Debbah, "Drone small cells in the clouds: Design, deployment and performance analysis," in *Proc. IEEE Global Commun. Conf. (GLOBECOM)*, Dec. 2015, pp. 1–6.

[17] R. I. Bor-Yaliniz, A. El-Keyi, and H. Yanikomeroglu, "Efficient 3-D placement of an aerial base station in next generation cellular networks," in *Proc. IEEE Int. Conf. Commun. (ICC)*, Kuala Lumpur, Malaysia, May 2016, pp. 1–5.

[18] L. Gupta, R. Jain, and G. Vaszkun, "Survey of important issues in UAV communication networks," *IEEE Commun. Surveys Tuts.*, vol. 18, no. 2, pp. 1123–1152, 2nd Quart., 2016.

[19] V. Sharma, M. Bennis, and R. Kumar, "UAV-assisted heterogeneous networks for capacity enhancement," *IEEE Commun. Lett.*, vol. 20, no. 6, pp. 1207–1210, Jun. 2016.

[20] E. Kalantari, H. Yanikomeroglu, and A. Yongacoglu, "On the number and 3D placement of drone base stations in wireless cellular networks," in *Proc. IEEE Veh. Technol. Conf. (VTC-Fall)*, Montreal, QC, Canada, Sep. 2016, pp. 1–6.

[21] M. O. Hasna and M. S. Alouini, "Optimal power allocation for relayed transmissions over Rayleigh-fading channels," *IEEE Trans. Wireless Commun.*, vol. 3, no. 6, pp. 1999–2004, Nov. 2004.

[22] T. Wang, A. Cano, G. B. Giannakis, and J. N. Laneman, "High-performance cooperative demodulation with decode-and-forward relays," *IEEE Trans. Commun.*, vol. 55, no. 7, pp. 1427–1438, Jul. 2007.

[23] G. Kramer, M. Gastpar, and P. Gupta, "Cooperative strategies and capacity theorems for relay networks," *IEEE Trans. Inf. Theory*, vol. 51, no. 9, pp. 3037–3063, Sep. 2005.

[24] İ. E. Telatar, "Capacity of multi-antenna Gaussian channels," *Eur. Trans. Telecommun.*, vol. 10, no. 6, pp. 585–595, 1999. [Online]. Available: http://dx.doi.org/10.1002/ett.4460100604

[25] V. Tarokh, N. Seshadri, and A. R. Calderbank, "Space-time codes for high data rate wireless communication: Performance criterion and code construction," *IEEE Trans. Inf. Theory*, vol. 44, no. 2, pp. 744–765, Mar. 1998.

[26] L. Zheng and D. N. C. Tse, "Diversity and multiplexing: A fundamental tradeoff in multiple-antenna channels," *IEEE Trans. Inf. Theory*, vol. 49, no. 5, pp. 1073–1096, May 2003.

[27] B. Wang, J. Zhang, and A. Høst-Madsen, "On the capacity of MIMO relay channels," *IEEE Trans. Inf. Theory*, vol. 51, no. 1, pp. 29–43, Jan. 2005.

[28] T. Kong and Y. Hua, "Optimal design of source and relay pilots for MIMO relay channel estimation," *IEEE Trans. Signal Process.*, vol. 59, no. 9, pp. 4438–4446, Sep. 2011.

[29] M. Qingyu, A. Osseiran, and G. Jiansong, "MIMO amplify-and-forward relaying: Spatial gain and filter matrix design," in *Proc. IEEE Int. Conf. Commun. Workshops (ICC Workshops)*, Beijing, China, May 2008, pp. 26–30.

[30] A. S. Behbahani, R. Merched, and A. M. Eltawil, "Optimizations of a MIMO relay network," *IEEE Trans. Signal Process.*, vol. 56, no. 10, pp. 5062–5073, Oct. 2008.

[31] Y. Rong, X. Tang, and Y. Hua, "A unified framework for optimizing linear nonregenerative multicarrier MIMO relay communication systems," *IEEE Trans. Signal Process.*, vol. 57, no. 12, pp. 4837–4851, Dec. 2009.

[32] P. Kolodzy, "Spectrum policy task force," Federal Commun. Commission, Washington, DC, USA, Tech. Rep. ET Docket no. 02-135, Nov. 2002.

[33] J. Mitola and G. Q. Maguire, Jr., "Cognitive radio: Making software radios more personal," *IEEE Pers. Commun.*, vol. 6, no. 4, pp. 13–18, Apr. 1999.

[34] A. Goldsmith, S. A. Jafar, I. Maric, and S. Srinivasa, "Breaking spectrum gridlock with cognitive radios: An information theoretic perspective," *Proc. IEEE*, vol. 97, no. 5, pp. 894–914, Apr. 2009.

[35] S. Haykin, "Cognitive radio: Brain-empowered wireless communications," *IEEE J. Sel. Areas Commun.*, vol. 23, no. 2, pp. 201–220, Feb. 2005.

[36] S. M. Perlaza, N. Fawaz, S. Lasaulce, and M. Debbah, "From spectrum pooling to space pooling: Opportunistic interference alignment in MIMO cognitive networks," *IEEE Trans. Signal Process.*, vol. 58, no. 7, pp. 3728–3741, Jul. 2010.

[37] X. Kang, R. Zhang, Y.-C. Liang, and H. K. Garg, "Optimal power allocation strategies for fading cognitive radio channels with primary user outage constraint," *IEEE J. Sel. Areas Commun.*, vol. 29, no. 2, pp. 374–383, Feb. 2011.

[38] L. Sboui, H. Ghazzai, Z. Rezki, and M.-S. Alouini, "Achievable rate of cognitive radio spectrum sharing MIMO channel with space alignment and interference temperature precoding," in *Proc. IEEE Int. Conf. Commun. (ICC)*, Budapest, Hungary, Jun. 2013, pp. 2656–2660.

[39] L. Sboui, H. Ghazzai, Z. Rezki, and M.-S. Alouini, "Achievable rate of spectrum sharing cognitive radio multiple-antenna channels," *IEEE Trans. Wireless Commun.*, vol. 14, no. 9, pp. 4847–4856, Sep. 2015.

[40] G. Zhao *et al.*, "Spatial spectrum holes for cognitive radio with relay-assisted directional transmission," *IEEE Trans. Wireless Commun.*, vol. 8, no. 10, pp. 5270–5279, Oct. 2009.

[41] L. Li, X. Zhou, H. Xu, G. Y. Li, D. Wang, and A. Soong, "Simplified relay selection and power allocation in cooperative cognitive radio systems," *IEEE Trans. Wireless Commun.*, vol. 10, no. 1, pp. 33–36, Jan. 2011.

[42] C. Gong, G. Yue, and X. Wang, "A transmission protocol for a cognitive bidirectional shared relay system," *IEEE J. Sel. Topics Signal Process.*, vol. 5, no. 1, pp. 160–170, Feb. 2011.

[43] L. Sboui, H. Ghazzai, Z. Rezki, and M.-S. Alouini, "On the throughput of a relay-assisted cognitive radio MIMO channel with space alignment," in *Proc. 12th Int. Symp. Workshops Modeling Optim. Mobile, Ad Hoc Wireless Netw. (WiOpts)*, Hammamet, Tunisia, May 2014, pp. 311–317.

[44] L. Sboui, H. Ghazzai, Z. Rezki, and M.-S. Alouini, "Achievable rate of multi-relay cognitive radio MIMO channel with space alignment," in *Proc. 10th Int. Conf. Cognit. Radio Oriented Wireless Netw. (Crowncom)*, Doha, Qatar, Apr. 2015, pp. 17–29.

[45] X. Bai, "Space alignment based on primary transmission-outage for cognitive transmission," *Electron. Lett.*, vol. 48, no. 19, pp. 1213–1214, Sep. 2012.

[46] D. Hamza and S. Aissa, "An optimal probabilistic multiple-access scheme for cognitive radios," *IEEE Trans. Veh. Technol.*, vol. 61, no. 7, pp. 3002–3014, Sep. 2012.

[47] L. Sboui, H. Ghazzai, Z. Rezki, and M. S. Alouini, "Achievable rate of a cognitive MIMO multiple access channel with multi-secondary users," *IEEE Commun. Lett.*, vol. 19, no. 3, pp. 403–406, Mar. 2015.

[48] I. Krikidis, B. Rong, and A. Ephremides, "Network-level cooperation for a multiple-access channel via dynamic decode-and-forward," *IEEE Trans. Inf. Theory*, vol. 57, no. 12, pp. 7759–7770, Dec. 2011.

[49] J. Yang and S. Ulukus, "Delay-minimal transmission for average power constrained multi-access communications," *IEEE Trans. Wireless Commun.*, vol. 9, no. 9, pp. 2754–2767, Sep. 2010.

[50] "Extending LTE advanced to unlicensed spectrum," Qualcomm Incorporated, San Diego, CA, USA, Tech. Rep., Dec. 2013. [Online]. Available: https://www.qualcomm.com/media/documents/files/white-paper-extending-lte-advanced-to-unlicensed-spectrum.pdf

[51] W. Qi, W. Hou, L. Guo, Q. Song, and A. Jamalipour, "A unified routing framework for integrated space/air information networks," *IEEE Access*, vol. 4, pp. 7084–7103, 2016.

[52] P. Popovski, H. Yomo, K. Nishimori, R. Di Taranto, and R. Prasad, "Opportunistic interference cancellation in cognitive radio systems," in *Proc. 2nd IEEE Int. Symp. New Frontiers Dyn. Spectr. Access Netw. (DySPAN)*, Dublin, Ireland, Apr. 2007, pp. 472–475.

[53] J. Gorski, F. Pfeuffer, and K. Klamroth, "Biconvex sets and optimization with biconvex functions: A survey and extensions," *Math. Methods Oper. Res.*, vol. 66, no. 3, pp. 373–407, Dec. 2007.

[54] Y. Li and M. Chen, "Software-defined network function virtualization: A survey," *IEEE Access*, vol. 3, pp. 2542–2553, 2015.

[55] L. Sboui, H. Ghazzai, Z. Rezki, and M.-S. Alouini, "Precoder design and power allocation for MIMO cognitive radio two-way relaying systems," *IEEE Trans. Commun.*, vol. 64, no. 10, pp. 4111–4120, Oct. 2016.

[56] E. Biglieri, A. J. Goldsmith, L. J. Greenstein, N. B. Mandayam, and H. V. Poor, *Principles of Cognitive Radio*. Cambridge, U.K.: Cambridge Univ. Press, 2012.
[57] S. M. Perlaza, M. Debbah, S. Lasaulce, and J.-M. Chaufray, "Opportunistic interference alignment in MIMO interference channels," in *Proc. 19th IEEE Int. Symp. Pers., Indoor Mobile Radio Commun. (PIMRC)*, Cannes, France, Sep. 2008, pp. 1–5.
[58] S. Boyd and L. Vandenberghe, *Convex Optimization*. Cambridge, U.K.: Cambridge Univ. Press, 2004.
[59] L. Sboui, Z. Rezki, and M. S. Alouini, "A unified framework for the ergodic capacity of spectrum sharing cognitive radio systems," *IEEE Trans. Wireless Commun.*, vol. 12, no. 2, pp. 877–887, Feb. 2013.
[60] X. Tang and Y. Hua, "Optimal design of non-regenerative MIMO wireless relays," *IEEE Trans. Wireless Commun.*, vol. 6, no. 4, pp. 1398–1407, Apr. 2007.
[61] V. A. Ubhaya, "Quasi-convex optimization," *J. Math. Anal. Appl.*, vol. 116, no. 2, pp. 439–449, 1986.
[62] B. Bereanu, "Quasi-convexity, strictly quasi-convexity and pseudo-convexity of composite objective functions," *Revue française d'automatique, informatique, recherche opérationnelle. Mathématique*, vol. 6, no. 1, pp. 15–26, 1972.
[63] L. Armijo, "Minimization of functions having Lipschitz continuous first partial derivatives," *Pacific J. Math.*, vol. 16, no. 1, pp. 1–3, 1966.

LOKMAN SBOUI (S'11) was born in Cairo, Egypt. He received the Dipl.Ing. degree (Hons.) from the Ecole Polytechnique de Tunisie, La Marsa, Tunisia, in 2011, and the M.S. degree from the King Abdullah University of Science and Technology, in 2013, where he is currently pursuing the Ph.D. degree in electrical engineering. His current research interests include performance of cognitive radio systems, MIMO, UAV, low SNR communications, relaying performances, energy efficient power allocation, and green wireless sensor networks.

HAKIM GHAZZAI (S'12–M'15) was born in Tunisia. He received the Diplome d'Ingenieur Master of Science degree in telecommunication engineering from the Ecole Superieure des Communications de Tunis (SUP'COM), Tunisia, in 2010 and 2011, respectively. He received the Ph.D degree in electrical engineering from King Abdullah University of Science and Technology (KAUST), Saudi Arabia, in 2015. He is currently working as a Research Scientist with Qatar Mobility Innovations Center (QMIC), Doha, Qatar. He was a recipient of appreciation for an exemplary reviewer of the *IEEE Wireless Communications Letters* in 2016. His general research interests include mobile and wireless networks, green communications, internet of things, and UAV-based communications.

ZOUHEIR REZKI (SM'08) was born in Casablanca, Morocco. He received the Dipl.Ing. degree from the École Nationale de l'Industrie Minérale , Rabat, Morocco, in 1994, the M.Eng. degree from the École de Technologie Supérieure, Montreal, QC, Canada, in 2003, and the Ph.D. degree from École Polytechnique, Montreal, QC, in 2008, all in electrical engineering. From 2008 to 2009, he was a post-Doctoral Research Fellow with the Data Communications Group, Department of Electrical and Computer Engineering, The University of British Columbia. From 2009 to 2016, he was a Research Scientist with the King Abdullah University of Science and Technology, Thuwal, Saudi Arabia. He is currently an Assistant Professor with the University of Idaho, Moscow, ID, USA. His current research interests include: performance limits of communication systems, cognitive and sensor networks, physical-layer security, and low-complexity detection algorithms.

MOHAMED-SLIM ALOUINI (S'94–M'98–SM'03–F'09) was born in Tunis, Tunisia. He received the Ph.D. degree in electrical engineering from the California Institute of Technology, Pasadena, CA, USA, in 1998. He served as a Faculty Member with the University of Minnesota, Minneapolis, MN, USA, then with the Texas A&M University at Qatar, Doha, Qatar, before joining King Abdullah University of Science and Technology, Thuwal, Saudi Arabia, as a Professor of Electrical Engineering in 2009. His current research interests include the modeling, design, and performance analysis of wireless communication systems.